

Intrinsic rotation due to non-Maxwellian equilibria in tokamak plasmas

Jungpyo (J.P.) Lee (Part 1)

Michael Barnes (Part 2)

Felix I. Parra

MIT Plasma Science & Fusion Center.

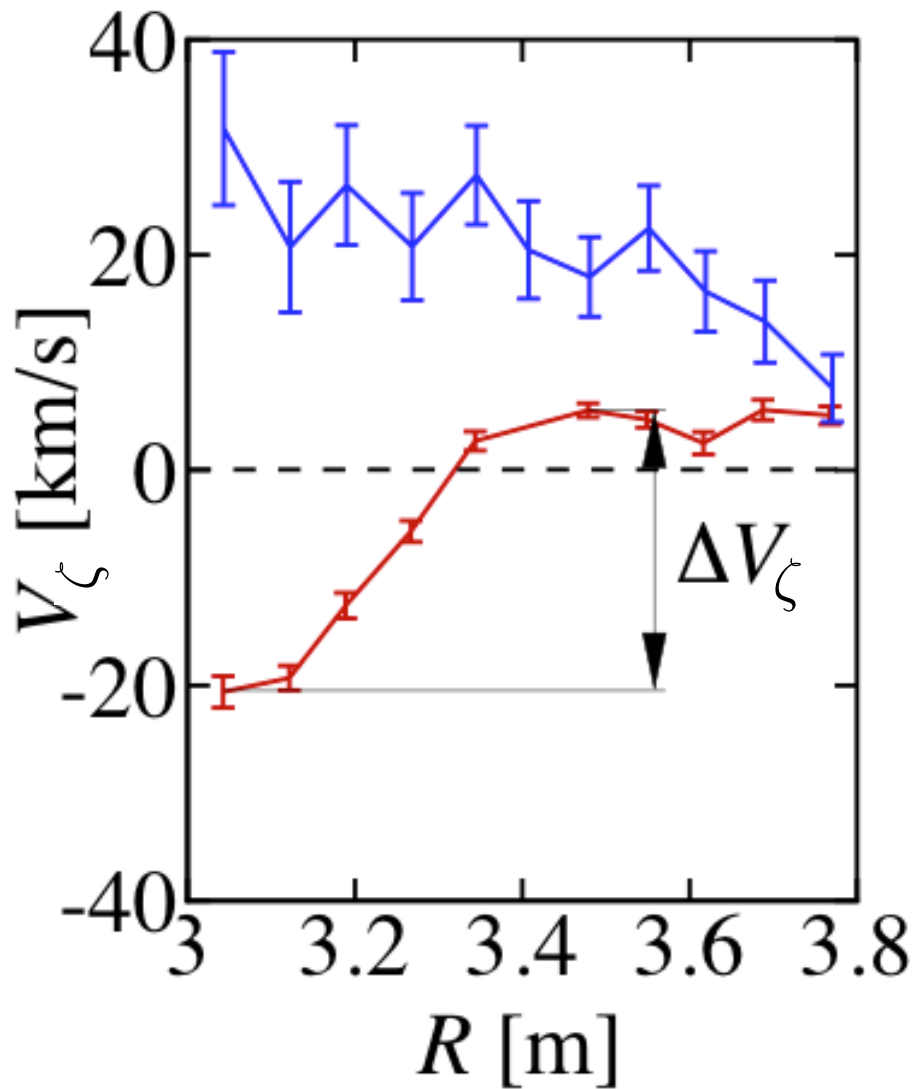
Outlines

- Introduction to intrinsic rotation
- Part 1: Turbulent momentum pinch of diamagnetic flows → Peaked rotation profile due to strong pedestal in H-mode
- Part 2: Sign reversal of the momentum transport by non-Maxwellian equilibria → From peaked to hollow profile due to the change in collisionality

Introduction

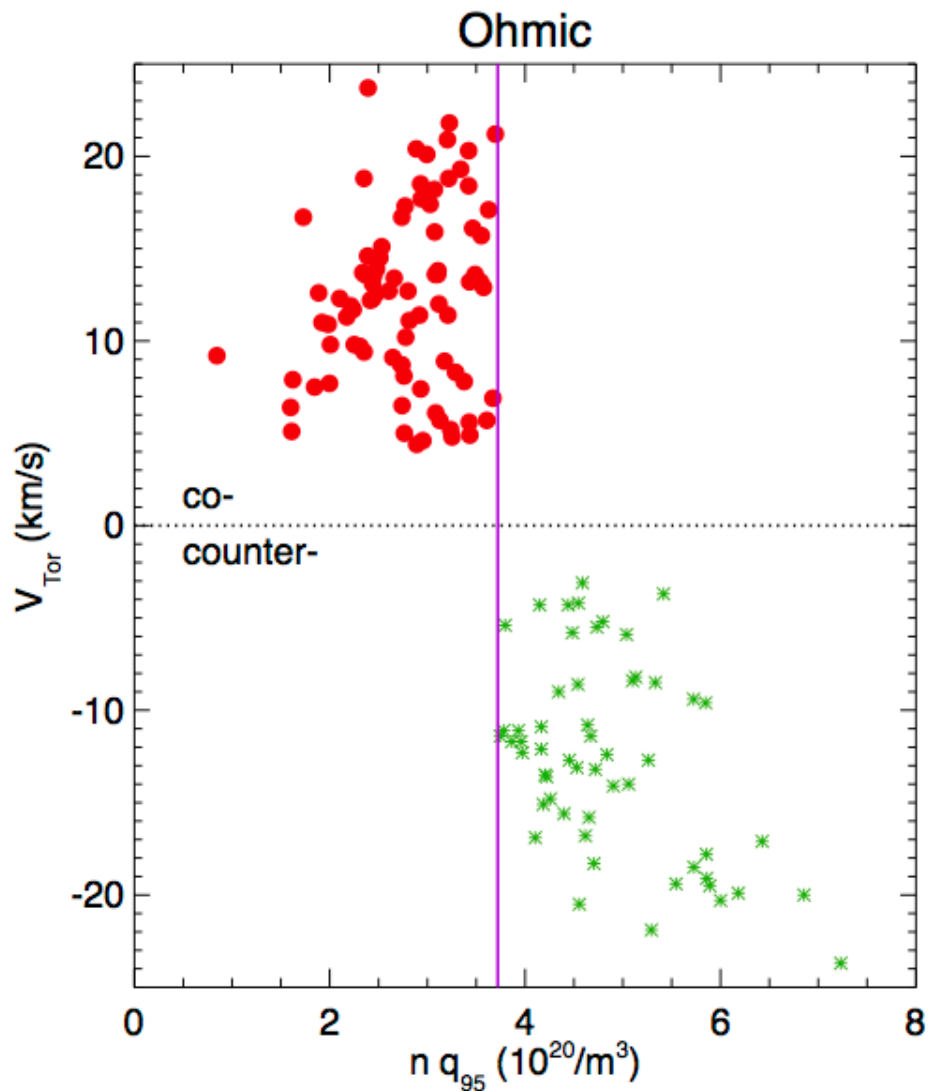
Measurement of intrinsic toroidal rotation (1)

- H-mode: peaked profile in the co-current direction
- L-mode: both peaked and hollow profiles
- A sign change at mid-radius due to an internal momentum redistribution
- Low flow regime (subsonic)



Measurement of intrinsic toroidal rotation (2)

- Ohmic : Rotation reversal from co-current direction to counter-current direction (peaked → hollow) by changing plasma parameters (increased density or decreased plasma current)



Rice et al.(2011) NF

Intrinsic momentum transport determines the radial profile of rotation

- Without external source, the radial transport of the toroidal angular momentum is

$$\Pi = \underbrace{\Pi_{int}}_{\neq 0} - \underbrace{P_\zeta n_i m_i R V_\zeta}_{\text{pinch}} - \underbrace{\chi_\zeta n_i m_i R \frac{\partial V_\zeta}{\partial r}}_{\text{diffusion}} = 0$$

Intrinsic momentum transport determines the radial profile of rotation

- Without external source, the radial transport of the toroidal angular momentum is

$$\Pi = \underbrace{\Pi_{int}}_{\neq 0} - \underbrace{P_\zeta n_i m_i R V_\zeta}_{\text{pinch}} - \underbrace{\chi_\zeta n_i m_i R \frac{\partial V_\zeta}{\partial r}}_{\text{diffusion}} = 0$$

$$\rightarrow V_\zeta(0) = V_\zeta(a) \exp\left(\frac{P_\zeta}{\chi_\zeta} r\right) - \int_{r=0}^{r=a} \frac{\Pi_{int}}{n_i m_i R} \exp\left(\frac{P_\zeta}{\chi_\zeta} r\right)$$

- Fixed velocity boundary condition at $r=a$:
Momentum source and sink at the wall

Intrinsic momentum transport determines the radial profile of rotation

- Without external source, the radial transport of the toroidal angular momentum is

$$\Pi = \underbrace{\Pi_{int}}_{\neq 0} - \underbrace{P_\zeta n_i m_i R V_\zeta}_{\text{pinch}} - \underbrace{\chi_\zeta n_i m_i R \frac{\partial V_\zeta}{\partial r}}_{\text{diffusion}} = 0$$

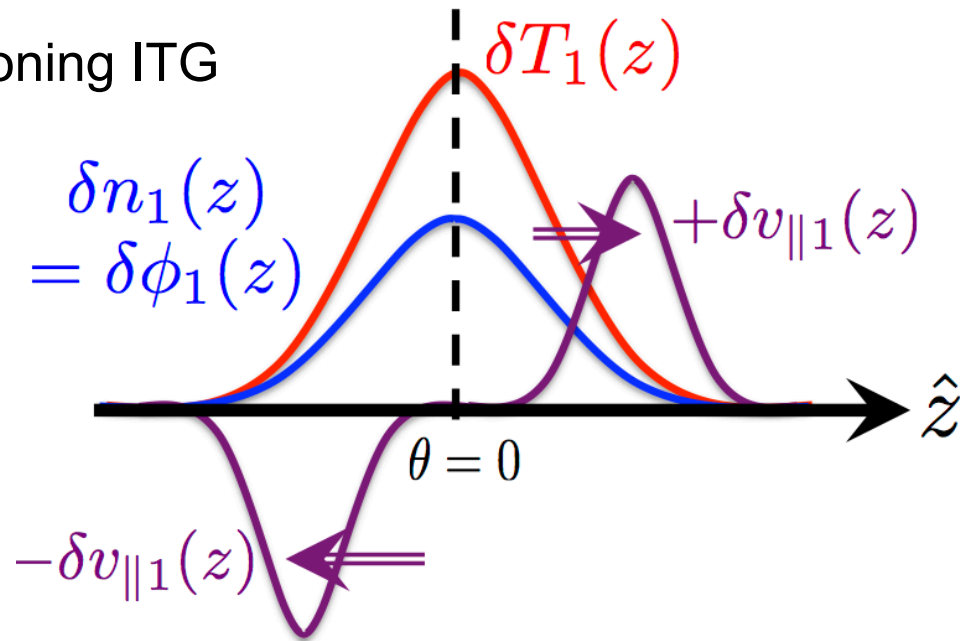
$$\rightarrow V_\zeta(0) = V_\zeta(a) \exp\left(\frac{P_\zeta}{\chi_\zeta} r\right) - \int_{r=0}^{r=a} \frac{\Pi_{int}}{n_i m_i R} \exp\left(\frac{P_\zeta}{\chi_\zeta} r\right)$$

- Fixed velocity boundary condition at $r=a$:
Momentum source and sink at the wall
- Inward pinch $P_\zeta > 0$ and diffusion out $\chi_\zeta > 0$
- The sign of intrinsic flux at outer radius determines the velocity direction in the core
(If $\Pi(V = 0, \partial V / \partial r = 0) > 0$ around the edge, then $V(r = 0) < 0$)

No intrinsic momentum flux in the lowest order

- No intrinsic toroidal angular momentum flux in the lowest order for an up-down symmetric tokamak

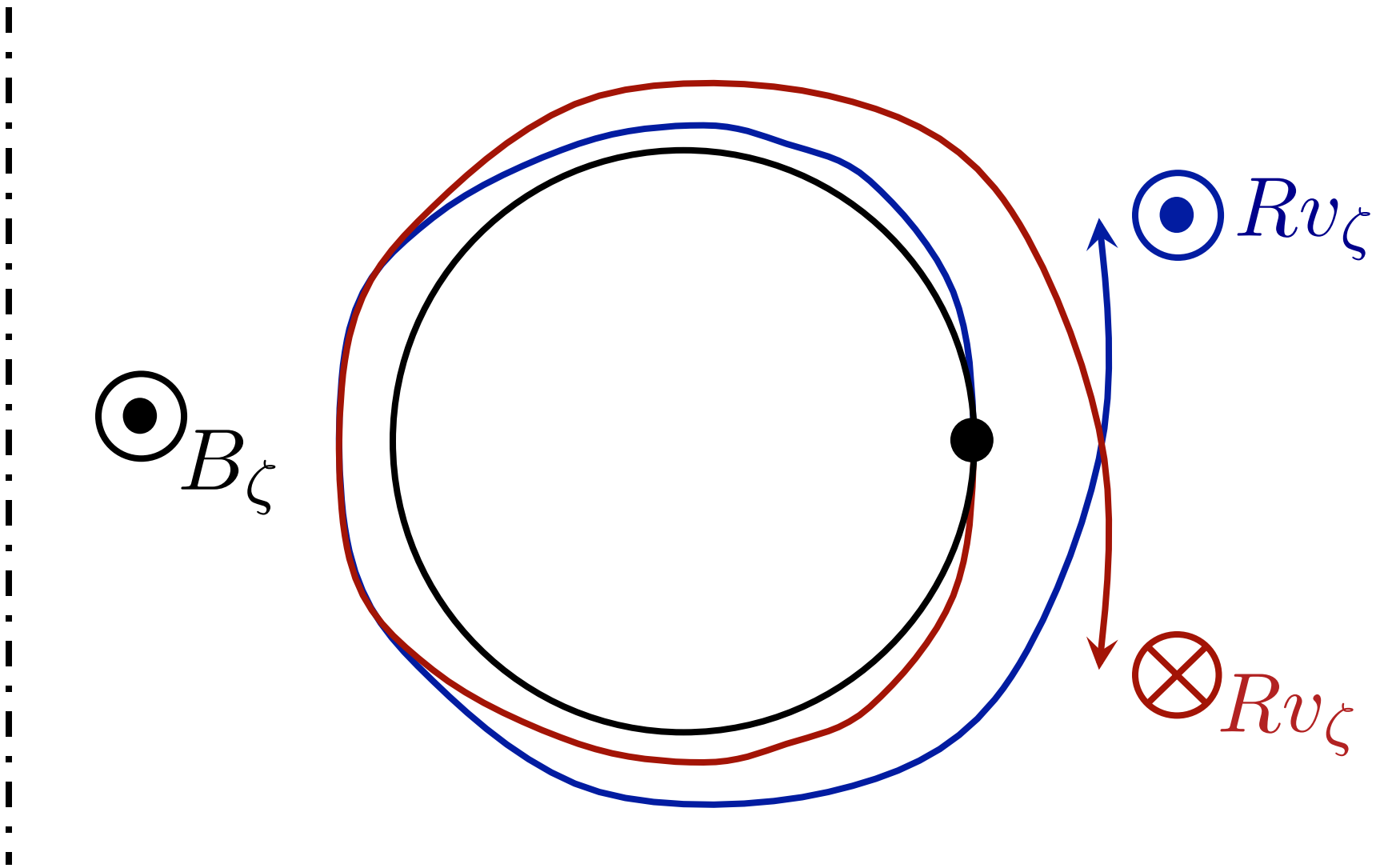
Example: ballooning ITG



$$\Pi_1(\theta, v_{\parallel}, k_x) = -\Pi_1(-\theta, -v_{\parallel}, -k_x)$$

where $\Pi_1 \propto \text{Re}[ik_y \phi_1^* h_1 v_{\parallel}]$ *Parra et. al. PoP (2011)*

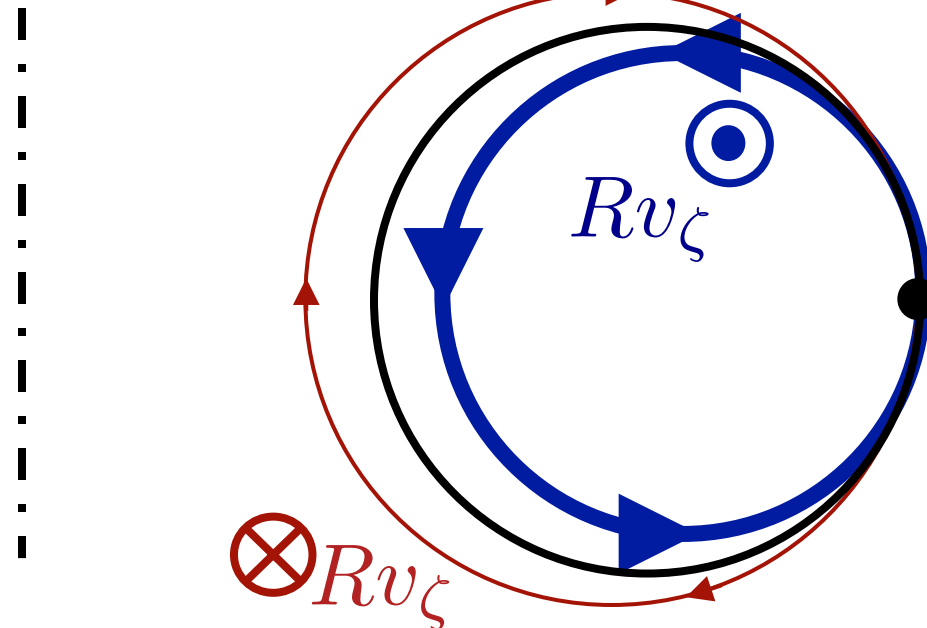
Symmetry of the momentum transport



Types of intrinsic momentum transport

- Phenomena that break the symmetry
 - Up-down asymmetric tokamak
 - Global profile effect on turbulence
 - Neoclassical flow effect on turbulence

$$u_s \propto \Delta r \frac{d \ln p}{dr} v_{th} \sim \frac{B}{B_\theta} \frac{\rho}{L_p} v_{th}$$



Higher-order effects in Gyrokinetic equation

$$\begin{aligned} \frac{dg_s}{dt} + \mathbf{v}_{\parallel} \cdot \nabla \left(g_s - Z_s e \langle \Phi \rangle \frac{\partial F_{0s}}{\partial E} \right) &+ \langle \mathbf{v}_E^{\perp} \rangle \cdot \nabla F_{0s} \\ &+ (\mathbf{v}_{Cs} + \mathbf{v}_{Ms} + \langle \mathbf{v}_E^{\perp} \rangle) \cdot \nabla_{\perp} \left(g_s - Z_s e \langle \Phi \rangle \frac{\partial F_{0s}}{\partial E} \right) \\ = -\mathbf{v}_{Ms} \cdot \nabla \theta \frac{\partial}{\partial \theta} \left(g_s - Z_s e \langle \Phi \rangle \frac{\partial F_{0s}}{\partial E} \right) &- \langle \mathbf{v}_E^{\parallel} \rangle \cdot \nabla_{\perp} g_s \\ - \langle \mathbf{v}_E^{\perp} \rangle \cdot \nabla \theta \frac{\partial g_s}{\partial \theta} &- \langle \mathbf{v}_E^{\parallel} \rangle \cdot \nabla F_{0s} - \langle \mathbf{v}_E^{\perp} \rangle \cdot \nabla F_{1s} \\ + Z_s e (\mathbf{v}_{\parallel} \cdot \nabla \langle \Phi \rangle + \mathbf{v}_{Ms} \cdot \nabla_{\perp} \langle \Phi \rangle) \left(\frac{\partial g_s}{\partial E} + \frac{\partial F_{1s}}{\partial E} \right) & \\ - \mathbf{v}_E^{nc} \cdot \nabla_{\perp} g_s + Z_s e \mathbf{v}_{\parallel} \cdot \nabla \Phi^{nc} \frac{\partial g_s}{\partial E} &+ \psi\text{-profile variation} \end{aligned}$$

Neoclassical parallel heat flow can also break the symmetry of turbulence

- Neoclassical distribution function in the higher order distribution function :

$$F_1 = F_1^{u\parallel} + F_1^{q\parallel} + F_1^{other} \sim \frac{B}{B_\theta} \rho^* F_0$$

Neoclassical parallel heat flow can also break the symmetry of turbulence

- Neoclassical distribution function in the higher order distribution function :

$$F_1 = F_1^{u\parallel} + F_1^{q\parallel} + F_1^{other} \sim \frac{B}{B_\theta} \rho^* F_0$$

- Neoclassical parallel particle flow piece:

$$F_1^{u\parallel} = \frac{mv_{\parallel}u_{\parallel}}{T} F_0 \quad \text{where} \quad u_{\parallel} \left(\frac{\partial p}{\partial r}, \frac{\partial T}{\partial r}, \nu^* \right) = \frac{1}{n} \int dv^3 v_{\parallel} F_1^{u\parallel}$$

Neoclassical parallel heat flow can also break the symmetry of turbulence

- Neoclassical distribution function in the higher order distribution function :

$$F_1 = F_1^{u\parallel} + F_1^{q\parallel} + F_1^{other} \sim \frac{B}{B_\theta} \rho^* F_0$$

- Neoclassical parallel particle flow piece:

$$F_1^{u\parallel} = \frac{mv\parallel u\parallel}{T} F_0 \quad \text{where} \quad u\parallel \left(\frac{\partial p}{\partial r}, \frac{\partial T}{\partial r}, \nu^* \right) = \frac{1}{n} \int dv^3 v\parallel F_1^{u\parallel}$$

- Neoclassical parallel heat flow piece:

$$F_1^{q\parallel} = \frac{2}{5} \frac{mv\parallel q\parallel}{PT} \left(\frac{mv^2}{2T} - \frac{5}{2} \right) F_0 \quad \text{where} \quad q\parallel \left(\frac{\partial p}{\partial r}, \frac{\partial T}{\partial r}, \nu^* \right) = \frac{1}{n} \int dv^3 v\parallel \frac{mv^2}{2} F_1^{q\parallel}$$

Neoclassical parallel heat flow can also break the symmetry of turbulence

- Neoclassical distribution function in the higher order distribution function :

$$F_1 = F_1^{u\parallel} + F_1^{q\parallel} + F_1^{other} \sim \frac{B}{B_\theta} \rho^* F_0$$

- Neoclassical parallel particle flow piece:

$$F_1^{u\parallel} = \frac{mv\parallel u\parallel}{T} F_0 \quad \text{where} \quad u\parallel \left(\frac{\partial p}{\partial r}, \frac{\partial T}{\partial r}, \nu^* \right) = \frac{1}{n} \int dv^3 v\parallel F_1^{u\parallel}$$

- Neoclassical parallel heat flow piece:

$$F_1^{q\parallel} = \frac{2}{5} \frac{mv\parallel q\parallel}{PT} \left(\frac{mv^2}{2T} - \frac{5}{2} \right) F_0 \quad \text{where} \quad q\parallel \left(\frac{\partial p}{\partial r}, \frac{\partial T}{\partial r}, \nu^* \right) = \frac{1}{n} \int dv^3 v\parallel \frac{mv^2}{2} F_1^{q\parallel}$$

$$\Pi \left(F_1, \frac{\partial F_1}{\partial r}, \dots \right) \rightarrow \Pi \left(\frac{\partial p}{\partial r}, \frac{\partial T}{\partial r}, \nu^*, \frac{\partial^2 p}{\partial r^2}, \frac{\partial^2 T}{\partial r^2}, \frac{\partial \nu^*}{\partial r}, \dots \right)$$

Part 1. Turbulent momentum pinch of diamagnetic flows

Momentum transport for ExB flow and diagnagnetic flow are different

- There are two types of toroidal rotation (Assume small poloidal rotation)

$$\Omega_\zeta = \underbrace{-c \frac{\partial \phi_0}{\partial \psi}}_{E \times B \text{ flow}} - \underbrace{\frac{c}{Z \epsilon n_i} \frac{\partial p_i}{\partial \psi}}_{\text{diamagnetic flow}}$$

- Difference between two types of rotation

Toroidal rotation source	Origin	Time scale	Effects on particle motion
Radial electric fields	Force balance	Momentum transport	Change in orbit and energy
Pressure gradient	Energy and particle transport	Energy transport	No change in orbit and energy. Only particle flux difference

Intrinsic momentum transport occurs when two types of rotations cancel each other

- Different pinch and diffusion coefficients for two types of rotation generate intrinsic momentum transport

$$\Pi = \Pi'_{int} - m_i R^2 [P_{\zeta,E} \Omega_{\zeta,E} + P_{\zeta,p} \Omega_{\zeta,p}] - m_i R^2 \left[\chi_{\zeta,E} \frac{\partial \Omega_{\zeta,E}}{\partial r} + \chi_{\zeta,p} \frac{\partial \Omega_{\zeta,p}}{\partial r} \right]$$

Intrinsic momentum transport occurs when two types of rotations cancel each other

- Different pinch and diffusion coefficients for two types of rotation generate intrinsic momentum transport

$$\begin{aligned}\Pi = & \Pi'_{int} - m_i R^2 [P_{\zeta,E} \Omega_{\zeta,E} + P_{\zeta,p} \Omega_{\zeta,p}] - m_i R^2 \left[\chi_{\zeta,E} \frac{\partial \Omega_{\zeta,E}}{\partial r} + \chi_{\zeta,p} \frac{\partial \Omega_{\zeta,p}}{\partial r} \right] \\ = & \underbrace{\left[\Pi'_{int} - m_i R^2 \left(\frac{P_{\zeta,E} - P_{\zeta,p}}{2} \right) (\Omega_{\zeta,E} - \Omega_{\zeta,p}) - m_i R^2 \left(\frac{\chi_{\zeta,E} - \chi_{\zeta,p}}{2} \right) \left(\frac{\partial \Omega_{\zeta,E}}{\partial r} - \frac{\partial \Omega_{\zeta,p}}{\partial r} \right) \right]}_{\Pi_{int}} \\ & - \left[m_i R^2 \left(\frac{P_{\zeta,E} + P_{\zeta,p}}{2} \right) (\Omega_{\zeta,E} + \Omega_{\zeta,p}) \right] - \left[m_i R^2 \left(\frac{\chi_{\zeta,E} + \chi_{\zeta,p}}{2} \right) \left(\frac{\partial \Omega_{\zeta,E}}{\partial r} + \frac{\partial \Omega_{\zeta,p}}{\partial r} \right) \right]\end{aligned}$$

Intrinsic momentum transport occurs when two types of rotations cancel each other

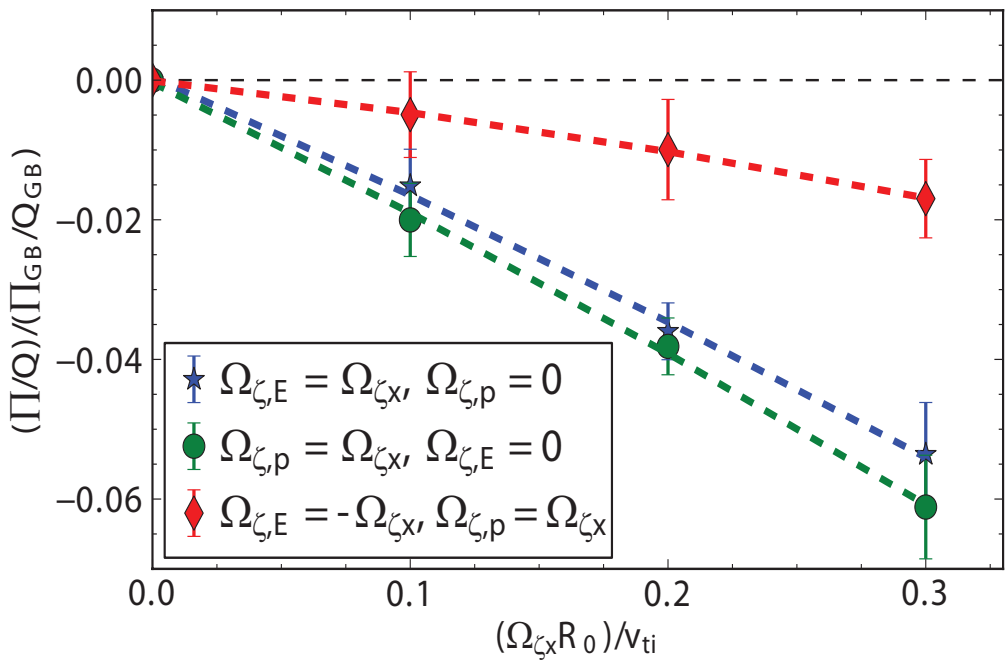
- Different pinch and diffusion coefficients for two types of rotation generate intrinsic momentum transport

$$\begin{aligned}\Pi = & \Pi'_{int} - m_i R^2 [P_{\zeta,E} \Omega_{\zeta,E} + P_{\zeta,p} \Omega_{\zeta,p}] - m_i R^2 \left[\chi_{\zeta,E} \frac{\partial \Omega_{\zeta,E}}{\partial r} + \chi_{\zeta,p} \frac{\partial \Omega_{\zeta,p}}{\partial r} \right] \\ = & \underbrace{\left[\Pi'_{int} - m_i R^2 \left(\frac{P_{\zeta,E} - P_{\zeta,p}}{2} \right) (\Omega_{\zeta,E} - \Omega_{\zeta,p}) - m_i R^2 \left(\frac{\chi_{\zeta,E} - \chi_{\zeta,p}}{2} \right) \left(\frac{\partial \Omega_{\zeta,E}}{\partial r} - \frac{\partial \Omega_{\zeta,p}}{\partial r} \right) \right]}_{\Pi_{int}} \\ & - \left[m_i R^2 \left(\frac{P_{\zeta,E} + P_{\zeta,p}}{2} \right) (\Omega_{\zeta,E} + \Omega_{\zeta,p}) \right] - \left[m_i R^2 \left(\frac{\chi_{\zeta,E} + \chi_{\zeta,p}}{2} \right) \left(\frac{\partial \Omega_{\zeta,E}}{\partial r} + \frac{\partial \Omega_{\zeta,p}}{\partial r} \right) \right]\end{aligned}$$

 $\Pi_{int} = \left(\frac{\partial p_i}{\partial r}, \frac{\partial^2 p_i}{\partial r^2} \right)$

Momentum pinch for diamagnetic flow is bigger than that for a ExB flow

The ratio of momentum pinch
($\Pi = -P_\zeta m_i R^2 \Omega_\zeta$) to heat flux



- Linearity on the rotation holds
- Different factors of rotation peaking due to the momentum pinches

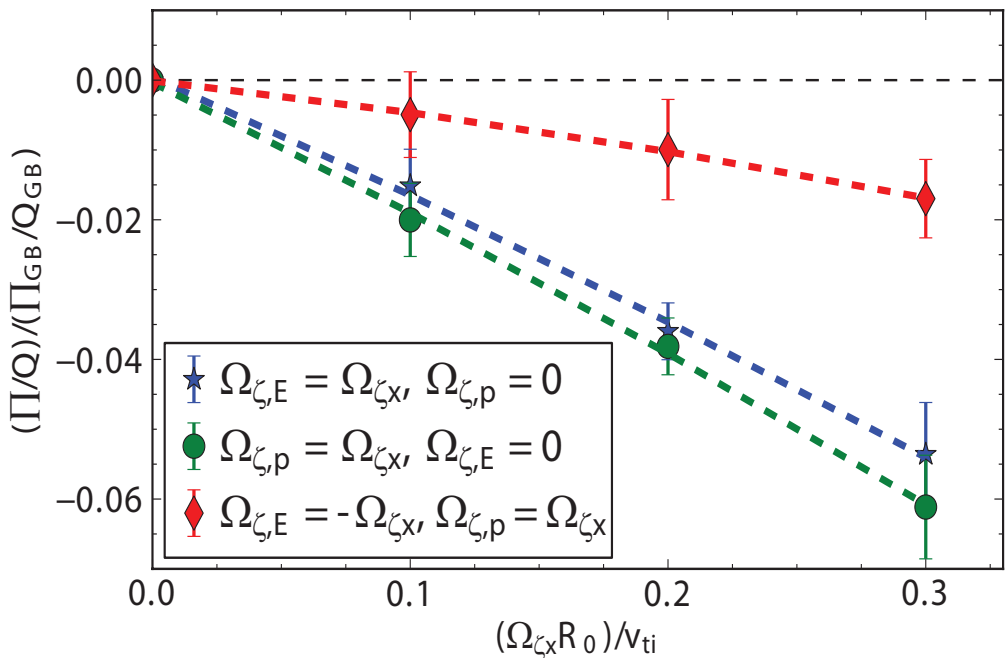
$$-\frac{1}{\Omega_\zeta} \frac{\partial \Omega_\zeta}{\partial r} = \frac{P_\zeta}{\chi_\zeta}$$

$R/L_T = 9.0, R/L_n = 9.0, q = 2.5, r/a = 0.8, R/a = 3.0, \hat{s} = 0.8$

$$Pr \equiv \frac{\chi_\zeta}{\chi_i} = 0.517$$

Momentum pinch for diamagnetic flow is bigger than that for a ExB flow

The ratio of momentum pinch
($\Pi = -P_\zeta m_i R^2 \Omega_\zeta$) to heat flux



$$R/L_T = 9.0, R/L_n = 9.0, q = 2.5, r/a = 0.8, R/a = 3.0, \hat{s} = 0.8$$

$$Pr \equiv \frac{\chi_\zeta}{\chi_i} = 0.517$$

- Linearity on the rotation holds
- Different factors of rotation peaking due to the momentum pinches
 - Radial electric field driven $P_{\zeta,E}/\chi_\zeta \simeq 2.9/R_0$
 - Pressure gradient driven $P_{\zeta,p}/\chi_\zeta \simeq 3.5/R_0$

Gyrokinetic equations are different for different type of rotations

- In lab frame, there is an additional acceleration term due to the radial electric field → Origin of the different pinches: the energy of the particle changes not by pressure gradient but by radial electric field

$$\frac{\partial f_{tb}^{(L)}}{\partial t} + \left(v_{\parallel} \hat{b} + \mathbf{v}_M + \frac{c}{B} \nabla(\phi_0 + \langle \phi^{tb} \rangle) \times \hat{b} \right) \cdot \nabla f_{tb}^{(L)} - \boxed{\frac{Ze}{m_i} \mathbf{v}_M \cdot \nabla \phi_0 \frac{\partial f_{tb}^{(L)}}{\partial E}}$$
$$= \frac{c}{B} \nabla \langle \phi^{tb} \rangle \times \hat{b} \cdot \nabla f_0^{(L)} + \frac{Ze}{m_i} [v_{\parallel} \hat{b} + \mathbf{v}_M] \cdot \nabla \langle \phi^{tb} \rangle \frac{\partial f_0^{(L)}}{\partial E} + C(f_i)$$

Gyrokinetic equations are different for different type of rotations

- In lab frame, there is an additional acceleration term due to the radial electric field → Origin of the different pinches: the energy of the particle changes not by pressure gradient but by radial electric field

$$\frac{\partial f_{tb}^{(L)}}{\partial t} + \left(v_{\parallel} \hat{b} + \mathbf{v}_M + \frac{c}{B} \nabla(\phi_0 + \langle \phi^{tb} \rangle) \times \hat{b} \right) \cdot \nabla f_{tb}^{(L)} - \boxed{\frac{Ze}{m_i} \mathbf{v}_M \cdot \nabla \phi_0 \frac{\partial f_{tb}^{(L)}}{\partial E}}$$

$$= \frac{c}{B} \nabla \langle \phi^{tb} \rangle \times \hat{b} \cdot \nabla f_0^{(L)} + \frac{Ze}{m_i} [v_{\parallel} \hat{b} + \mathbf{v}_M] \cdot \nabla \langle \phi^{tb} \rangle \frac{\partial f_0^{(L)}}{\partial E} + C(f_i)$$

- In the frame rotating with total toroidal flow, $\Omega_{\zeta} = \Omega_{\zeta,E} + \Omega_{\zeta,p}$ the Coriolis terms due to the total flow, but energy correction due to $\Omega_{\zeta,p}$

$$\left(\frac{\partial}{\partial t} + \Omega_{\zeta} R \hat{\zeta} \cdot \nabla \right) f_{tb}^{(R)} + \left(v_{\parallel} \hat{b} - \frac{\Omega_{\zeta,p}}{B} \hat{b} \times \nabla \psi + \mathbf{v}_M + \mathbf{v}_C - \frac{c}{B} \nabla \langle \phi^{tb} \rangle \times \hat{b} \right) \cdot \nabla f_{tb}^{(R)}$$

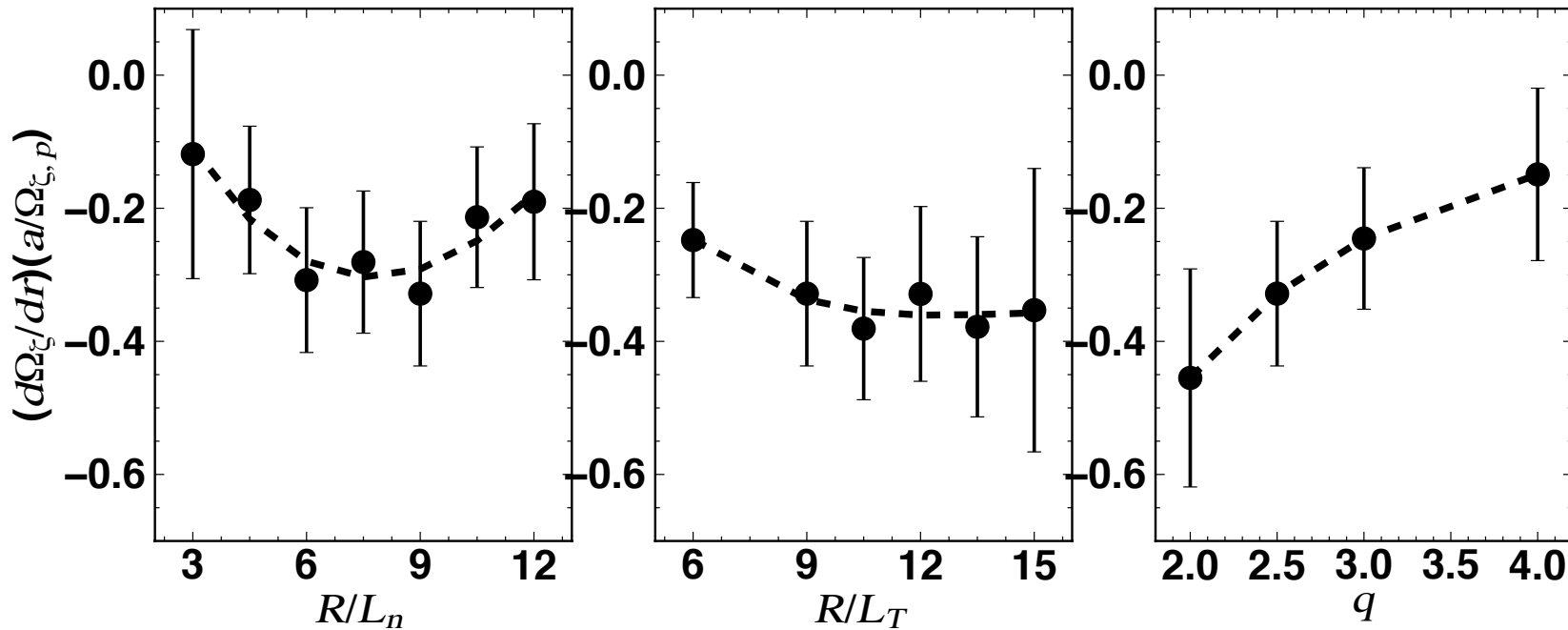
$$- \boxed{\frac{Ze}{m_i c} \Omega_{\zeta,p} \mathbf{v}_M \cdot \nabla \psi \frac{\partial f_{tb}^{(R)}}{\partial \varepsilon}} = \frac{c}{B} \nabla \langle \phi^{tb} \rangle \times \hat{b} \cdot \nabla f_0^{(R)} + \frac{Ze}{m_i} [v_{\parallel} \hat{b} + \mathbf{v}_M + \mathbf{v}_C] \cdot \nabla \langle \phi^{tb} \rangle \frac{\partial f_0^{(R)}}{\partial \varepsilon} + C(f_i)$$

Where $\mathbf{v}_C = \frac{2v_{\parallel}\Omega_{\zeta}}{\Omega_i} \hat{b} \times [(\nabla R \times \zeta) \times \hat{b}]$ is the drift due to the Coriolis force.

Rotation peaking due to positive diamagnetic flow and negative ExB flow varies by parameters

Rotation peaking ($\Pi < 0$) when $\Omega_\zeta = \Omega_{\zeta,E} + \Omega_{\zeta,p} = 0$

($\Omega_{\zeta,E}R = -0.3$ and $\Omega_{\zeta,p}R = 0.3$)



Strong pressure gradient in the pedestal results in a large inward intrinsic momentum transport(H-mode)

- In the pedestal, a negative radial electric field is generated to balance the strong radial pressure drop

$$\Omega_{\zeta,E} \sim -\Omega_{\zeta,p} < 0$$

- Rotation peaking can be significant due to the strong pressure drop

(e.g. for a pedestal with $\Delta T_i \sim -1keV$, $\Delta r \sim 1cm$, and $B_\theta \sim 0.5T$

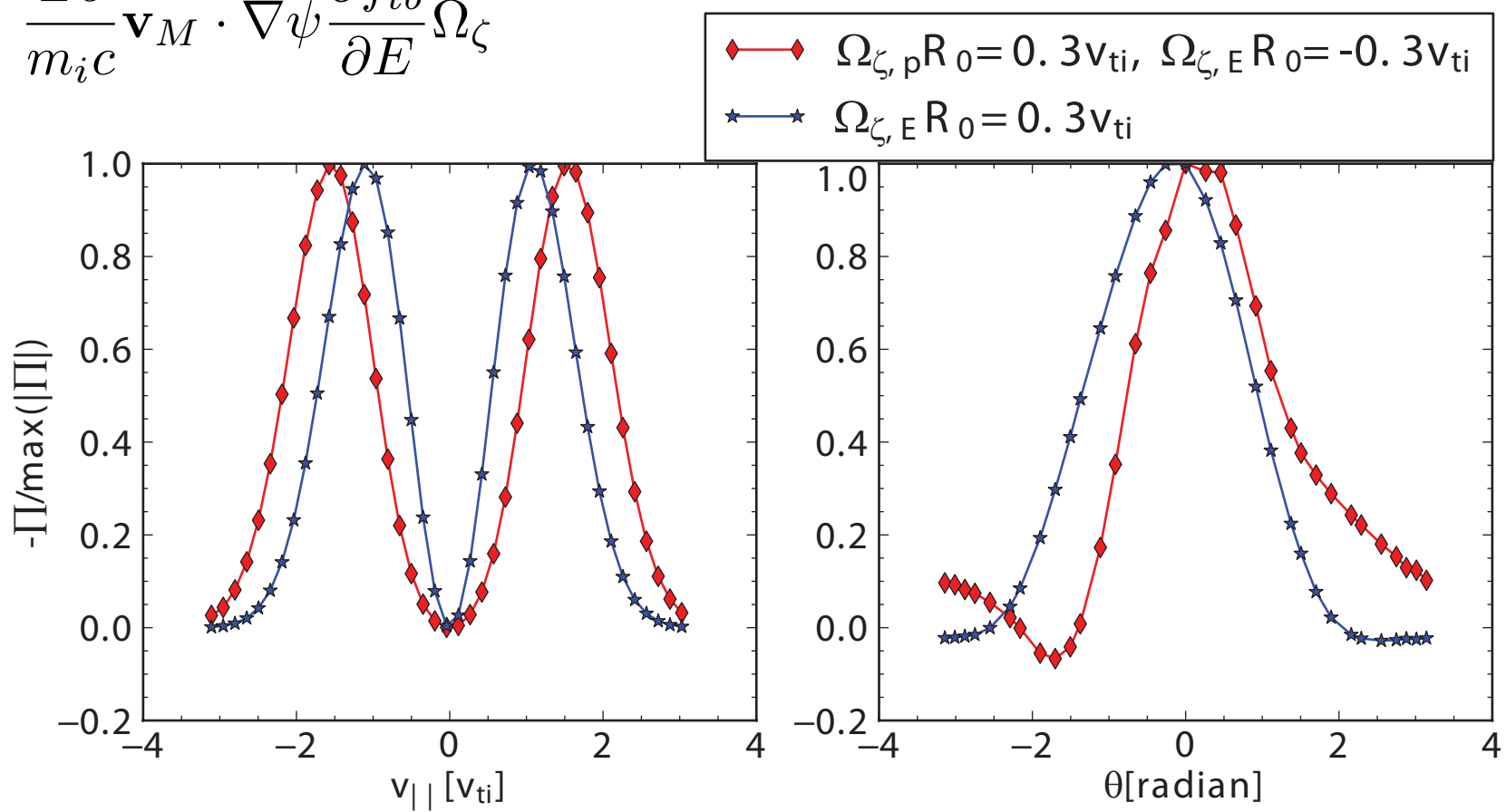
$$\rightarrow \Omega_{\zeta,p} R_0 \sim 200 \text{km/s at the pedestal}$$

$$\rightarrow \Omega_\zeta R_0 \sim -a \frac{\partial \Omega_\zeta}{\partial r} R_0 \sim 0.4 \Omega_{\zeta,p} R_0 \sim 80 \text{km/s at the core})$$

The acceleration due to radial electric field results in intrinsic momentum transport

- The difference between two momentum pinches are caused by acceleration term

$$\frac{Ze}{m_i c} \mathbf{v}_M \cdot \nabla \psi \frac{\partial f_{tb}}{\partial E} \Omega_\zeta$$



Part 2. Sign reversal of the momentum transport by non- Maxwellian equilibria